Water Research 292 (2026) 125313

Contents lists available at ScienceDirect

Water Research

journal homepage: www.elsevier.com/locate/watres

Extracellular polymeric substances in aerobic granular sludge under increasing salinity conditions

Le Min Chen [a,*], Sunanda Keisham [b], Hiroaki Tateno [b], Gijs Y. Kleine [a], Martin Pabst [a], Mario Pronk [a,c], Mark C.M. van Loosdrecht [a], Yuemei Lin [a]

[a] Department of Biotechnology, Delft University of Technology, Van der Maasweg 9, 2629 HZ Delft, the Netherlands
[b] Cellular and Molecular Biotechnology Research Institute, National Institute of Advanced Industrial Science and Technology (AIST), Tsukuba Ibaraki 305-8566, Japan
[c] Haskoning, Laan 1914 35, Amersfoort 3800 AL, the Netherlands

HIGHLIGHTS

- "*Ca.* Accumulibacter" is the dominant species from 1– 4 % salinity.
- The charge density of EPS and its charged glycoproteins increased with increasing salinity.
- Increasing salinity induces the upregulation of glycan biosynthesis genes.
- Putative glycoproteins produced by "*Ca.* Accumulibacter" were identified.
- Flagella, PEP-CTERM protein and autotransporter protein are putative glycoproteins.

GRAPHICAL ABSTRACT

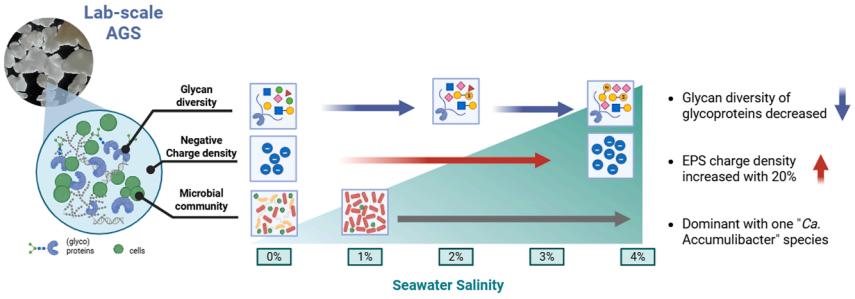

ARTICLE INFO

Keywords:
Extracellular polymeric substances
Aerobic granular sludge
Seawater
Glycoprotein
Charge density

ABSTRACT

The long-term effects of environmental conditions, such as seawater salinity, on the extracellular investigated EPS changes during a stepwise increase in salinity (0–4%), renewing over 90% of biomass at each condition. Stable granulation, complete anaerobic acetate uptake, and phosphate removal were maintained throughout. FT-IR of granules showed significant changes in glycans (1025 cm^{-1}) and sialic acid (1730 cm^{-1}), which were reflected in the EPS. Lectin microarray revealed that increasing salinity reduced glycan diversity in EPS glycoproteins, while increasing negatively charged groups, including sialic acids and sulfated groups. At 4% salinity, EPS negative charge increased by 19.8% compared to 0%. Microbial community composition shifted from a diverse mix (Dechloromonas; 23%, "*Candidatus* Competibacter"; 13%, "*Candidatus* Accumulibacter"; 28%) at 0% to a dominant (69% – 75%) unclassified Accumulibacter clade I species at 1 - 4% salinity. Metaproteomic analysis showed strong upregulation of genes of "*Ca.* Accumulibacter" involved in monosaccharide, lipopolysaccharide, and peptidoglycan biosynthesis from 3% - 4% salinity, indicating its adaptation to salinity stress. Dechloromonas and "*Ca.* Competibacter" represented a minor or a non-significant fraction of those proteins related to glycan synthesis across the salinities. Despite that no glycoprotein biosynthesis pathways were identified in the metaproteomic data, three putative glycoproteins produced by "*Ca.* Accumulibacter" were detected across all conditions. They were downregulated as the salinity increased. These findings highlight how "*Ca.* Accumulibacter" dynamically adapts its EPS, particularly glycoprotein glycans, in response to increasing salinity, offering new insights into EPS adaptation under environmental stress.

* Corresponding author.
E-mail address: L.M.Chen@tudelft.nl (L.M. Chen).

https://doi.org/10.1016/j.watres.2025.125313
Received 17 October 2025; Received in revised form 12 December 2025; Accepted 31 December 2025
Available online 9 January 2026

1. Introduction

Aerobic granular sludge (AGS) is a wastewater treatment process known for its robustness and efficiency (Pronk et al., 2015). With this technology, microorganisms grow in the form of compact granules where they are embedded in a self-produced matrix of extracellular polymeric substances (EPS) providing structural integrity and protection against various environmental factors. Among these factors, salinity has emerged as an important factor for the stability of AGS systems.

Salinity is one of the environmental factors increasingly affecting wastewater treatment systems, particularly in coastal cities. The daily usage of seawater for applications, such as flushing toilets, fire control, along with the discharge of high saline water from industrial wastewaters, can lead to the accumulation of high-salinity wastewater in treatment facilities, which can impact the sludge stability (Lefebvre and Moletta, 2006; Zhang et al., 2023). Despite several comprehensive studies on process performance, such as biological phosphate removal on seawater salinity (de Graaff et al., 2020), NaCl-induced salinity (Pronk et al., 2014; Wang et al., 2017; Welles et al., 2014) or alternating salinities (Hou et al., 2019), the understanding into corresponding changes in the EPS remain limited and contradictory. Some studies have reported that AGS cultivated under high saline conditions have shown to produce more EPS (Corsino et al., 2017) and proteins (Campo et al., 2018; Ou et al., 2018), whereas others have observed elevated polysaccharides content in the EPS at alternating salinities (Hou et al., 2019). While these studies provide some general insight into the adaptations in the EPS against saline conditions, it remains unclear which EPS components produced are being modified by the microorganisms during the adaptation. The EPS generally consists of polysaccharides, proteins, extracellular enzymes and diverse glycoconjugates, such as lipopolysaccharides and glycoproteins (Seviour et al., 2019). In particular, glycoproteins have recently gained more attention as an EPS component of AGS as they may play important structural and functional roles within the granule matrix (Chen et al., 2023b; de Graaff et al., 2019; Páez-Watson et al., 2024).

Protein glycosylation is one of the most common post-translational modifications found in nature and was long believed to be exclusive to eukaryotes (Schäffer and Messner, 2017). However, it is now recognized as widespread in bacteria and archaea, functioning in protein stabilization, cell motility and biofilm formation (Eichler and Koomey, 2017; Nothaft and Szymanski, 2010). While the understanding on the bacterial protein glycosylation pathways and functions are largely based on studies of pathogenic model species (*Campylobacter jejuni* and *Haemophilus influenzae)* (Eichler and Koomey, 2017), recent work has shown the presence and diversity of glycoproteins in environmental microbial communities. For example, a dense array produced by two different of glycans were found on the surface-layer proteins of an anaerobic ammonium oxidizing bacterium, as identified from an enrichment culture (Pabst et al., 2022). In a microbial community enriched with "*Candidatus* Accumulibacter", glycans of glycoproteins in the EPS were found highly diverse (Páez-Watson et al., 2024). Interestingly, other studies have shown that the pathways and chemical composition of glycoproteins are altering against the change in the environment, *i.e.* two distinct protein N-glycosylation pathways in *Haloferax volcanii* are differentially regulated by salinity (Kaminski et al., 2013). A short-term exposure to the saline condition results in variation of the glycan composition of AGS glycoproteins (Chen et al., 2023b). Those findings imply that there is a strong correlation between protein glycosylation and the varying of salinity. However, what this correlation is, including why and how salinity affects protein glycosylation patterns remains unclear.

To investigate the relationship between salinity, charge and protein glycosylation regulation in aerobic granular sludge, granules were cultured under seawater conditions with stepwise increasing salinity from 0% to 4%. At each salinity, the EPS was extracted from the biomass and changes in glycoprotein composition were analyzed using lectin microarray. The charge density of the EPS was determined using conductometric titration. Metaproteomics was employed to assess the microbial community composition and changes, explore potential glycosylation pathways and identify putative glycoproteins. Finally, a discussion was included on potential of multi-omics approaches to study protein glycosylation in granular sludge.

2. Material and methods

2.1. Reactor operation and monitoring the adaptation of granular sludge to the increasing seawater salinity

2.1.1. Reactor operation

A lab-scale bubble column with a working volume of 2.8 L (6.5 cm diameter) was operated as a sequencing batch reactor. The reactor was inoculated with 1:1 vol ratio of 600 mL sludge, consisting of activated sludge (Harnaschpolder, The Netherlands) and blended Nereda® sludge (Utrecht, the Netherlands). The temperature of the reactor was not directly controlled, but instead the room temperature was controlled at 20 °C. The dissolved oxygen (DO) was controlled through a mixture of air and nitrogen at 0% (anaerobic) and 80% (aerobic phase). The pH was controlled at a pH 7.3 ± 0.1 by dosing 1.0 M HCl or 1.0 M NaOH.

The salinity range (0 – 4%) was selected based on the typical concentrations of seawater (3.5%) intrusion in coastal wastewater systems resulting in brackish water (0.05 – 3%), such as in estuaries, and high-salinity streams from industrial brine discharges (1 – 15%) (Lefebvre and Moletta, 2006) or high-saline seas (*e.g.* Red sea, 4%). The synthetic wastewater consisted of 1.2 L of demiwater or increasing concentrations of artificial seawater (final concentration of 1%, 2%, 3% and 4% w/v Instant Ocean®), 150 mL medium A and 150 mL medium B. Medium A contained 62.5 mM $NaCH_3COO{\cdot}3H_2O$. Additional 3.6 mM $MgSO_4{\cdot}7H_2O$, and 4.7 mM KCl was added to medium A when mixed with demi water. $MgSO_4{\cdot}7H_2O$ and KCl were removed from the medium when using artificial seawater. Medium B was composed of 41.13 mM of NH_4Cl, 0.34 mM of K_2HPO_4, 0.27 mM of KH_2PO_4, 0.07 mM of allylthiourea to suppress nitrification and 10 mL of trace elements solution (Vishniac and Santer, 1957), but 2.2 g/L of $ZnSO_4{\cdot}7H_2O$ was used instead of 22 g/L and 2.18 g/L of $Na_2MoO_4{\cdot}2H_2O$ instead of $(NH_4)_6Mo_7O_{24}{\cdot}4H_2O$. The combination of medium A, B and the demi water or seawater, led to the final influent concentrations of 400 mg/L COD, 50 mg/L NH_4—N, and 12.2 mg/L PO_4-P. To monitor the reactor performance, samples were taken over the course of the cycle and filtered through a 0.22 μm PVDF filter. Phosphate and ammonia were measured using a Thermo Fisher Gallery Discrete Analyzer (Thermos Fisher Scientific, Waltham, USA). Acetate was measured through high-performance liquid chromatography (Thermo Scientific Vanquish HPLC) at 50 °C (0.75 mL/min) with 1.5 mM phosphoric acid as eluent and Aminex HPC-87H column (Bio-Rad, California, USA).

During the start-up, the settling phase was gradually decreased from 20 min to 3 min by monitoring the time required for the bed to set. Once stable granulation was formed the settling time was set at 3 min. The following reactor cycles were, 5 min effluent withdrawal, 5 min N_2 sparging, 5 min feeding with synthetic wastewater, 50 min anaerobic phase and 110 min of aerobic phase. Except for 4%, the anaerobic phase was 80 min and aerobic phase 160 min to ensure anaerobic acetate uptake and complete aerobic phosphate removal, respectively. The conductivity and the online profiles (DO, pH) were used to monitor the operation of the reactor. The volatile solids (*VS*) and ash fractions of the biomass were measured weekly of the granules and the effluent using the standard methods (APHA, 1998).

Stereo zoom pictures of the granules at the end of each salinity condition were taken with a stereo zoom microscope (M205 FA, Leica Microsystems, Germany) connected to the Eert Vision Auto Focus Microscope camera (Eert Vision, The Netherlands). The images were acquired with the Eert C304 software (V1.0, Eert Vision, The Netherlands).

The solid retention time (SRT) was controlled by manual sludge

Table 1
Overview of the duration, average SRT and newly grown biomass per condition. The % of new biomass calculated was done by using the average SRT: % new biomass = 1 - exp(-t / SRT), where t is the duration of the condition in days and SRT is the average SRT over that period.

% salinity	Duration (days)	Average SRT	% new biomass calculated
0	118	13	99.3
1	35	13	93.7
2	42	14	95.0
3	36	14	92.9
4	35	15	90.2

removal of the mixed liquid and recalculated each time based on the *VS*removed through sampling and effluent. During the start-up at fresh water condition (0% salinity), no sludge was removed for the first 52 days to allow the seed sludge to adapt to the new influent and reactor conditions . The overall SRT was maintained at 14 ± 1 days over the course of the experiment (Table 1). The salinity was increased stepwise. At each salinity, the duration was at least 35 days, about 2.5 SRTs in order to detect differences in the sludge. At least 90% of the biomass was renewed before taking the samples for EPS extraction and metaproteomic analysis.

For EPS analysis, the granules were taken at the end of the aerobic phase, rinsed with demi water to remove excess salt, lyophilized, and stored at room temperature. For the metaproteomic analysis, the granules were first pottered and washed three times with PBS. The biomass pellets were lyophilized before analysis.

2.1.2. Functional group analysis with Fourier transform – infrared spectroscopy

Biomass was taken throughout the experiment to monitor the general changes in the functional groups using Fourier transform-infrared spectroscopy (FT-IR). About 1 mL of granules were taken at the end of the aerobic phase and washed 3 times with 1 mL of demi water to remove the excess salt. The samples were immediately stored in the −80 °C and lyophilized for further analysis.

The lyophilized sample was crushed into a powder and measured on a Spectrum 100 spectrometer (PerkinElmer, Shelton, CT). The spectra were recorded in attenuated reflectance (ATR) mode at room temperature over a wavenumber range of 600 – 4000 cm^{-1} using 16 accumulations and a resolution of 1 cm^{-1}. The spectra were analyzed in OriginPro® (OriginLab, US). Normalization was performed on MATLAB on the wavenumber 1535 cm^{-1}, the amide II peak (Talari et al., 2016).

2.1.3. Sialic acid lectin staining of aerobic granular sludge

At each salinity, 1 mL of granules were collected and put into Eppendorf tubes washed with Milli-Q water for three times. The supernatant was carefully removed by spinning down the biomass using a small tabletop centrifuge at low speed. After washing, the samples were covered with a 500 μL of the MAA lectin solution (0.1 mg/mL) and incubated for 20 min in the dark at room temperature. Then, the samples were destained by carefully removing the unbound lectin by centrifuge at low speed. The supernatant was decanted, followed by adding 1 mL of tap water and carefully removed. The same washing steps were repeated three times. The destained sample was put on the glass slide, the cover slip was added on top of the biomass before imaging.

2.2. Monitoring the alteration of EPS properties in response to the increasing seawater salinity

2.2.1. EPS extraction and general analysis

About 350 mg of lyophilized granules (about 250 mg organic fraction, *VS*) were extracted in 25 mL 0.1 M NaOH (1% weight VS/volume) at 80 °C for 30 min in duplicate. The extracted mixture was cooled under running tap water and centrifuged at 3180 × *g* at 4 °C for 20 min. The supernatant was dialysed overnight to remove the excess salts against demi water using dialysis tubing (3.5 kDa molecular cut-off).

The total solids fraction of the dialysed EPS was determined using overnight drying at 105 °C, followed by burning at 550 °C to determine the *VS* fraction (APHA, 1998). The extracted and dialysed EPS was stored overnight at 4 °C. 100 mg equivalent of the total solids in volume was used for conductometric titration. The rest supernatant was frozen at −80 °C, lyophilized and stored at room temperature for further EPS analysis.

The lyophilized EPS was analyzed by FT-IR as described in section 2.1.2. The total protein content was determined by dissolving the lyophilized EPS in Milli-Q water to 1 mg/mL. The BCA protein assay was used following the manufacturer's instructions with bovine serum albumin as a standard (Pierce BCA protein assay Kit, Thermo Scientific). Protein absorbance was measured at 562 nm in triplicate using the multimode plate reader (TECAN Infinite M200 PRO, Männedorf, Switzerland).

2.2.2. The charge density of EPS analyzed by conductometric titration

The conductometric titration method was described in detail by Kleine et al. (2025). In short, one hundred mg equivalent of the total solids in the extracted EPS was diluted with demi water until a total volume of 50 mL. The solution was first set to pH 2 using 1 M HCl. The conductivity and pH curves were saved using LABVIEW 2014 SP1 (National Instruments). Afterwards, the solution was titrated to approximately pH 12 using a total of 1.5 ml 1 M NaOH with the set-up using a 765 dosimat (Metrohm, the Netherlands). During conductometric titration, pH and conductivity are measured simultaneously. As OH^- is dosed, it first neutralizes excess H^+ and then deprotonates functional groups like COOH and NH_3^+. These reactions create plateaus in the pH and conductivity curves, which can be used to calculate the sample's charge density (mmoles NaOH/gVS).

2.2.3. Glycan profiling of glycoproteins by lectin microarray

High-density lectin microarray was constructed according to the method described (Tateno et al., 2011). 0.4 μg protein eq. of lyophilized EPS was dissolved in 20 μL PBS-T and labeled with Cy3-N-hydroxysuccinimide ester (GE Health- care). Excess Cy3 was removed with Sephadex G-25 desalting columns (GE Healthcare) centrifuged at 1500 × *g* at 4 °C for 2 min. Cy3-labeled proteins were diluted with probing buffer (25 mM tris-HCl (pH 7.5), 140 mM NaCl, 2.7 mM KCl, 1 mM $CaCl_2$, 1 mM $MnCl_2$, and 1% Triton X-100) to 0.5 μg/mL and were incubated with the lectin microarray at 20 °C overnight. The lectin microarray was washed three times with probing buffer, and fluorescence images were captured using a Bio-Rex scan 200 evanescent-field-activated fluorescence scanner (Rexxam Co. Ltd., Kagawa, Japan). The samples were performed in technical duplicates on the duplicate EPS samples. The total fluorescence signal is normalized over each condition and visualized using Rstudio.

2.2.4. Detecting the glycan structure of the sialylated glycoproteins in the extracted EPS by combining lectin matrix prepacked column, enzymatic treatment and lectin microarray

Because aerobic granules cultivated with 4% salinity displayed the strongest sialic acid lectin staining signal (Supplementary Materials Fig. S1), the extracted EPS from the granules cultivated at this salinity was selected for the verification of the presence of sialic acid. The sialic acid-specific separopore®4B MAA lectin column (1 ml) was used for the purification of macromolecules containing sialic acid in the above extracted EPS according to the procedure provided by glycoMatrix™ (Dublin, OH). The collected fraction was lyophilized for further analysis.

High-density lectin microarray was generated according to the method described in 2.2.3. 0.4 μg of the MAA lectin column-enriched fraction was labeled with Cy3-N-hydroxysuccinimide ester (GE Healthcare), and excess Cy3 was removed with Sephadex G-25 desalting columns (GE Healthcare). 50 μL of Cy3-labelled sample was put into a separate tube and 0.5 μL of sialidase was added into the tube, mixed and

incubated at 37 °C for 1 h (in parallel, the probing buffer was treated in the same way as the control). The above Cy3-labeled MAA lectin column-enriched fraction with and without sialidase treatment were diluted with probing buffer (25 mM tris-HCl (pH 7.5), 140 mM NaCl, 2.7 mM KCl, 1 mM CaCl2, 1 mM MnCl2, and 1%Triton X-100) to 0.5 μg/mL and were incubated with the lectin microarray at 20 °C overnight. Further preparations and data visualization of the lectin microarray were performed as described in section 2.2.3.

2.3. Metaproteomic analysis

2.3.1. Protein extraction and digestion

The protein extraction was performed similar to Kleikamp et al. (2023). Hunderd fifty milligrams of acid washed glass beads (150–212 μm) with 170 μL of both TEAB and B-PER buffer was added to approximately six mg of the collected lyophilized biomass. The samples were homogenized using the bead beater for 2.5 min with 3 min incubation ice and repeated for a total of 3 cycles. Freeze/thaw cycles were performed by freezing the samples at −80 °C and thawing at 75 °C with centrifugation (1000 rpm, 5 min) for a total of 3 cycles. The supernatant volume was collected in a LoBind Eppendorf tube after centrifugation (20 min, 4 °C, 14,000 rcf). Protein precipitation was performed by addition of TCA at a ratio of 1:4 to the supernatant, vortexed and incubated at 4 °C for 30 min. The supernatant was removed after centrifugation (15 min, 4 °C, 14,000 rcf) and discarded. The protein pellets were washed with ice-cold acetone, spun down (3 min, 140,000 rcf) and the acetone was discarded. The pellets were reconstituted in 50 μL 6 M urea. The samples were reduced using 8.5 μL of 10 mM dithiothreitol (DTT) (60 min, 37 °C, 300 rpm), followed by alkylation using 8.5 μL of 20 mM iodoacetamide (IAA) by incubation for 60 min in the dark at room temperature. The samples were then diluted with 285 μL of 100 mM ammonium bicarbonate to obtain a urea concentration of < 1 M. Finally, 10 μL of 0.1 μg/μL trypsin (Promega) was added to the samples and incubated overnight at 37 °C. The obtained peptides were purified with a solid-phase extraction using Oasis HLB solid-phase extraction well plates (Waters) according to the protocol provided by the manufacturer. Purified peptide fractions were then dried in a SpeedVac concentrator and stored at −20 °C until further preparations for the analysis.

2.3.2. Shotgun metaproteomic analysis

The shotgun proteomic analysis was performed as described previously (Pabst et al., 2022), with changes as described in the following. An aliquot of each sample (corresponding to approx. 500 ng proteolytic digest) was analysed using a nano-liquid-chromatography system consisting of an EASY nano LC 1200 equipped with an Acclaim PepMap RSLC RP C18 reverse phase column (75 mm x 150 mm, 2 mm) coupled to a QE plus Orbitrap mass spectrometer (Thermo Scientific, Germany). Solvent A was H_2O containing 0.1% formic acid, and solvent B consisted of 80 % acetonitrile in H_2O, containing 0.1% formic acid. The flow rate was maintained at 350 nL/min. The Orbitrap was operated in top 10 data dependent acquisition (DDA) mode, acquiring peptide signals form 385–1250 m/z, at 70 K resolution in MS1 with an AGC target of 3e6 and max IT of 75 ms. The peptides were separated using a linear gradient from 5 to 25% B over 88 min, followed by a linear gradient to 55% B over 60 min. MS2 acquisition was performed at 17.5 K resolution, with an AGC target of 2e5, and a max IT of 75 ms, using a NCE of 28. Unassigned, singly charged as well as >5 charged mass peaks were excluded.

2.3.3. Processing of metaproteomic raw data

Mass spectrometric raw data were processed using PEAKS Studio X (Bioinformatics Solutions Inc., Canada) for database searching using the protein sequences identified from the contigs constructed from the whole metagenome sequencing data of the same samples including phage sequences, and the cRAP proteome (https://www.thegpm.org/crap/), allowing 20 ppm parent ion and 0.02 Da fragment mass error and up to 3 missed cleavages, oxidation/deamination as variable modifications and carbamidomethylation as fixed modification. Database search further used decoy fusion for estimation of false discovery rates (FDR) and subsequent filtering of peptide spectrum matches for 1% FDR, and 2 unique peptides per protein. Taxonomic classification of the identified proteins was performed using Diamond as described earlier (Kleikamp et al., 2023). Taxonomic composition was based on counting the number of matched peptides per taxonomic level (*e.g.* genus).

The annotation of protein functions was done using GhostKOALA to obtain KO numbers, and the R function keggGet (KEGG symbols). The number of detected peptides was normalized over the total abundance of each condition. The data was further processed in Rstudio; the protein abundances were normalized by Z-score normalization across the conditions and the library "pheatmap" was used for visualization. To determine the possible glycosylation sites, NetOGlyc 4.0.0.13 and NetNGlyc 1.0 were employed.

2.3.4. DNA extraction, sequencing and processing

DNA extraction was performed using the DNeasy® UltraClean® Microbial Kit (Qiagen, Germany) for the AGS samples grown in 0%, 1% and 2% salinity. For AGS grown under 3% and 4% salinity, PowerSoil Pro Kit (Qiagen, Germany) was used due to the low-quality DNA obtained with the DNeasy® UltraClean® Microbial Kit. The extracted DNA was quantified with a Qubit fluorometer and the quality of the DNA was measured on the TapeStation System (Agilent, Santa Clara, *CA*). Shotgun sequencing was performed on an Illumina NovaSeqX or NovaSeq600 platform (Hologenomix, NL).

Processing of the raw sequencing data was performed by Hologenomix (Delft, NL). The quality of the sequenced raw reads was assessed by FastQC (version 0.11.7) with default parameters (Andrews, 2010) and visualized with MultiQC (version 1.19). Low-quality paired-end reads were trimmed and filtered by Fastp version 0.23.4 on the paired-end mode (Chen, 2023). Taxonomic classification of raw reads was performed to profile the microbiome from each sample using the standard Kraken2 (version 2) database (uses all complete bacterial, archaeal, and viral genomes in NCBI Refseq database) complemented with a curated wastewater database (sludgeDB) with default tparameters (Wood et al., 2019). The taxonomic classification outcomes from Kraken2.0 were converted into abundance tables using the biom file converter tool and Pavian visualization tool (Breitwieser and Salzberg, 2020) to explore metagenomics classification datasets. To identify patterns in the microbiome, different types of ordination and statistical numerical methods were performed using the R software. The input data was the output of the taxonomic classification from Kraken2.0. Clean reads were assembled into contigs using MetaSPAdes (version 3.15.5) with default parameters (Nurk et al., 2017). Contigs resulting from the sequencing of only the iDNA pools of bioaggregates were binned with MetaBAT version 2.2.15 (Kang et al., 2019) to reconstruct metagenome-assembled genomes (MAGs or bins) on default parameters. The functional gene annotation process involved several steps. Firstly, Prokka version 1.14.5 was utilized to annotate the assembled sequences. This was executed in metagenomic mode, using the default databases and parameters as described by (Seemann, 2014). Subsequently, protein sequences were subjected to a two-step Diamond (version 2.1.8) blast search against the complete Uniprot database, encompassing Trembl and SwissProt (accessed the 10.09.2023). Initially, the search was conducted with default settings. Following this, a second search was performed using stringent parameters (e-value threshold of 0.0001, query coverage of 90%, and identity threshold of 90%). Upon identification of proteins through the Diamond blast searches, the headers of these proteins were replaced with the corresponding Prokka headers.

3. Results

3.1. Adaptation of granules towards increasing seawater salinity

The aerobic granular sludge reactor was seeded with freshwater based medium. After stable granulation was achieved, artificial seawater was used to prepare the medium. The salinity of the seawater (hereafter referred to as 'salinity') increased incrementally by 1 percentage point (1% w/v, equivalent to 10 g/L sea salt), reaching a final concentration of 4% (40 g/L sea salt). At each salinity condition, complete anaerobic acetate uptake and aerobic phosphate removal were observed. The entire biomass bed settled within 3 min. To ensure the long-term changes were captured, sampling of biomass was performed only after at least 90% of the biomass was renewed (2.5 SRT) at each salinity (Table 1). The morphology of the granules across all the saline conditions (from 0 - 4%) is shown in Fig. 1. The granules were compact with a smooth surface, and reached sizes between 0.5 – >3 mm.

Although the morphology of the granules was similar, there might be changes occurring in the functional groups of the biomass during the adaptation to the increasing salinity. To investigate this possibility, biomass was characterized by FTIR over the course of each salinity adaptation phase (Fig. 2). The main differences between the samples were observed in the intensity of the bands at 1025 cm^{-1} and 1730 cm^{-1}, which were assigned to the -C-O-C bond in glycans (carbohydrates) and the α-keto group of sialic acids (de Graaff et al., 2019; Talari et al., 2016). Notably, the variation tendency of these two bands was different: the absorbance intensity at 1025 cm^{-1} was first increasing from 1% to 2% salinity, afterwards a slight decrease from 2% to 3%, followed by a sharp decrease at 4%, representing a parabolic-like shape. While the absorbance intensity at 1730 cm^{-1} displayed the inverse trend, first a decrease from 1% to 2%, followed by a small increase from 2% to 3%, then a sharp increase at 4%. The band at 1730 cm^{-1} was assigned to α-keto group of sialic acids. To verify the presence of sialic acids in the granules, MAA lectin was employed to stain the granules. The MAA lectin binds sialic acids at the terminal sugar residue of glycan chains of glycoproteins (de Graaff et al., 2019). The signal of the lectin was weak for the 0% granules, while it became stronger with increasing salinity. The strongest signal was found for the 4% granules, indicated by a stronger red signal from the Cy5 labeled MAA lectin (Supplementary Materials Fig. S1). Both the FTIR and lectin staining results indicated a change in glycan composition (including sialic acids) during the adaptation of AGS to each salinity condition, despite that the morphology of AGS remained highly similar.

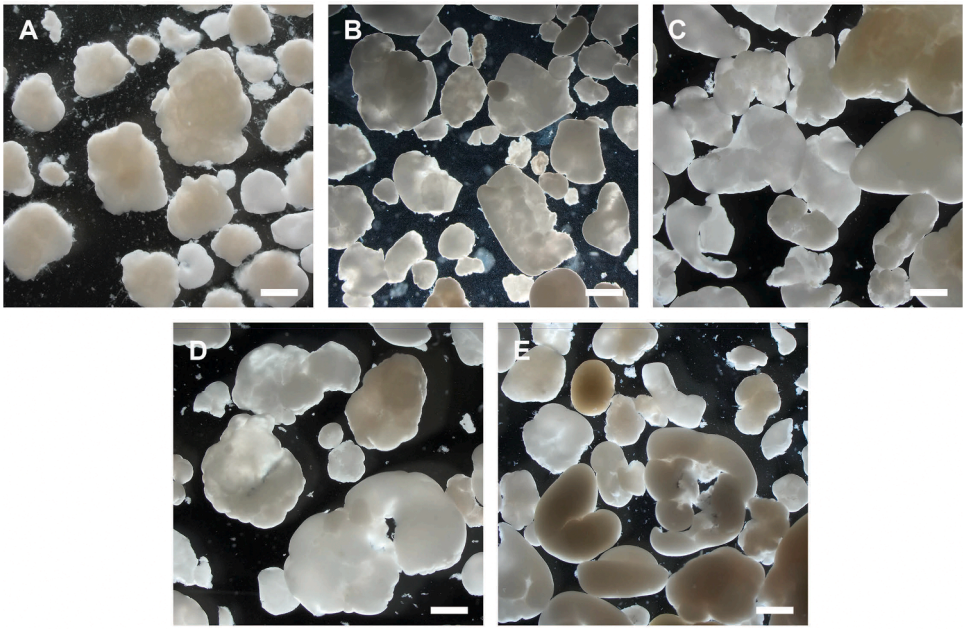

Fig. 1. Stereo zoom microscope pictures of the AGS grown under 0 % (A), 1 % (B), 2 % (C), 3 % (D) and 4 % (E). The scale bar indicates 1 mm.

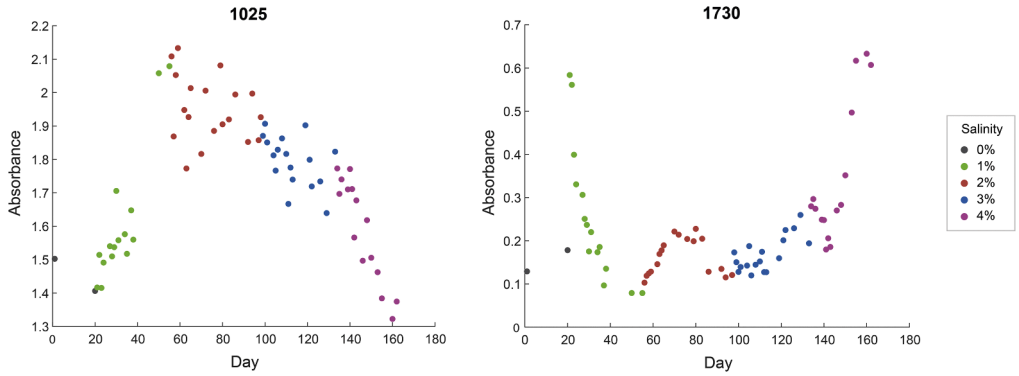

Fig. 2. Absorption of the normalized FT-IR peaks 1025 cm^{-1} (-C-O—C in carbohydrates) and 1730 cm^{-1} (α-keto acids of sialic acids) over the course of the increasing salinity.

Table 2
Overview of the EPS yield and protein content. EPS yield (g *VS* EPS/g VS granules). Protein content as determined by the BCA assay with BSA as a standard.

% salinity	Yield (g *VS* EPS /g VS Granules)	% Protein content (mg BSA eq./ mg EPS)
0	54.7 ± 0.9 %	42.7 ± 1.6 %
1	55.6 ± 0.3 %	36.6 ± 1.6 %
2	60.5 ± 2.9 %	36.5 ± 0.9 %
3	59.4 ± 0.5 %	38.2 ± 2.4 %
4	54.2 ± 3.6 %	39.1 ± 1.3 %

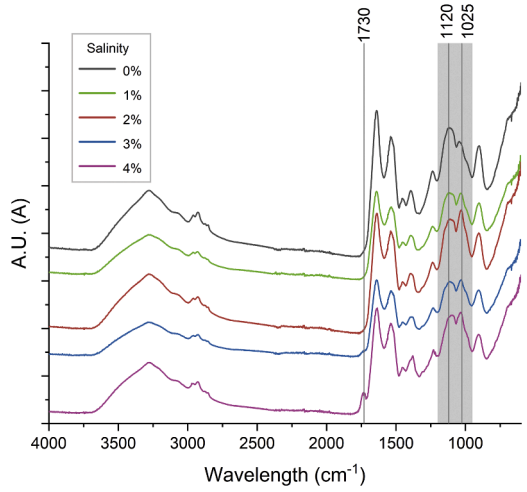

Fig. 3. FT-IR spectrum of the extracted EPS of the AGS exposed to different salinities. The shaded area (1200 – 900 cm^{-1}) represent functional groups related to carbohydrates (Talari et al., 2016).

3.2. General EPS characterization

To study whether the change in glycan composition is reflected in the EPS, the granules were collected at the end of each saline condition, and their EPS was extracted. As shown in Table 2, no significant differences were observed among the EPS yields. The protein content decreased by 5.9% from $EPS_{0\%}$ to $EPS_{1\%}$ and remained similar throughout the increasing salinity. When the functional groups of the EPS were examined by FT-IR, clear changes in the bands typical of carbohydrates were observed (Fig. 3), *i.e.* the peak of 1120 cm^{-1}, mostly representing C-O stretching of glycans (Talari et al., 2016), showed a strong peak at $EPS_{0\%}$ but shifted towards a broader peak with increasing salinity. The intensity of the peak at 1025 cm^{-1} (-C-O-C- bond in carbohydrates) increased relatively to that of 1120 cm^{-1}. The peak 1730 cm^{-1} (α-keto group of sialic acids) appeared at $EPS_{3\%}$ as a weak shoulder peak and became stronger at $EPS_{4\%}$. It seems that the glycans present in the EPS are altering in response to the increasing salinity, while there is a tendency for sialic acids to increase at higher salinity.

3.3. Comparative glycomics study

It is known that glycans include both free sugars (*e.g.* polysaccharides) and sugars attached to other molecules (*e.g.* sugars on glycoproteins and glycolipids) (Varki et al., 2017a). As protein glycosylation is one of the most abundant post-translational modifications, it impacts protein folding, stability and interactions (Nothaft and Szymanski, 2010). Glycoproteins in the EPS were specifically studied to understand their adaptation to salinity. To monitor the change of glycan-glycoprotein profile with salinity in the reactor, a lectin microarray was applied. Proteins were labeled with Cy3. If the proteins are glycosylated and the glycan profile matches the affinity of the lectins, a Cy3 signal will appear on the microarray. The intensity of the Cy3 signal reflects the relative abundance of glycoproteins, while the glycan patterns can be obtained from the specificity of lectins.

Among 96 lectins used, 90 gave a strong fluorescent binding signal across all EPS samples (Fig. 4), implying the presence of glycoproteins. These glycoproteins carried both N-linked glycosylation (indicated by lectins TxLcl, rXCL, CCA, and rSRL) and O-linked glycosylation (indicated by lectins HEA, MPA, VVA, and SBA). Those glycoproteins contained one or multiple glycans, such as sialic acids, lactosamine and/or polylactosamine, mannose, fucose, *N*-acetyl glucosamine, and galactose (with/without sulfation).

Interestingly, among the 5 EPS samples, $EPS_{0\%}$ showed the strongest binding for most lectins, indicating a higher glycan diversity (Fig. 4, indicated by the higher number of red-coloured blocks). Upon increasing to 1% salinity, a large number of lectins showed decreased signal intensities, including those binding to Man, GlcNAc, Fuc, βGalNAc. As the salinity increased, the glycan diversity decreased, with the lowest glycan diversity for $EPS_{4\%}$. However, the specific glycan trends differed: signals representing O-linked glycosylation increased with salinity, while those from N-linked glycosylation decreased. Specifically, the signal of a few sialic acid binding lectins (PVL, MAL, MAH, rACG) also appeared to increase with salinity.

To identify the most abundant glycan structures across EPS samples, the top 10 strongest signal of each EPS were visualized with their corresponding fluorescence intensity (Fig. 5). Across all samples, the most prevalent glycans contained structures carrying O-linked glycosylation, sialic acid, 6-sulfo-Gal, α1–6 fucose and mannose. As salinity increased, charged glycan structures became the most prominent. The signal representing binding of 6-sulfo-Gal (FLAG-EW29Ch-E20K) increased with

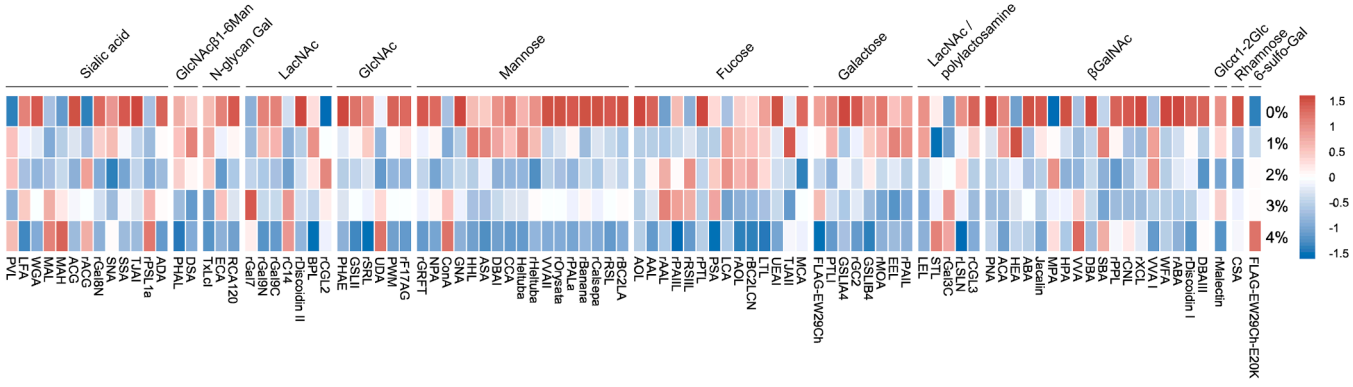

Fig. 4. Lectin microarray profile of the EPS over salinities (rows) min-max normalized for each lectin (columns). Red indicates higher-than-average binding intensity, and blue indicates lower-than-average intensity for each lectin. The specific structure of each lectin is indicated in the Supplementary Material Table S1. GlcNAc, N-acetylglucosamine; Man, mannose; Gal, galactose; LacNAc, N-acetylactosamine.

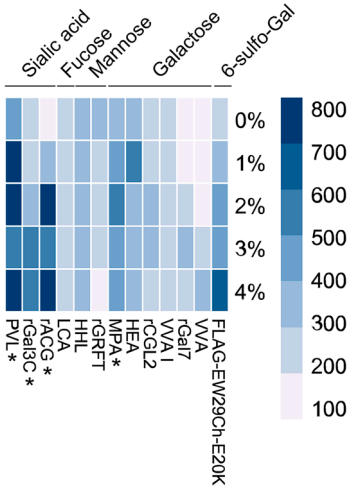

Fig. 5. Lectin microarray profile of the EPS over salinities (rows) for the top 10 lectins in each condition (columns). The darker the color represents the intensity of the signal, showing direct comparison of absolute binding across conditions. The lectin labeled with asterisk indicate the glycan structure of the enriched glycoprotein fraction of $EPS_{4\%}$ by MAA column (Supplementary Material Fig. S2).

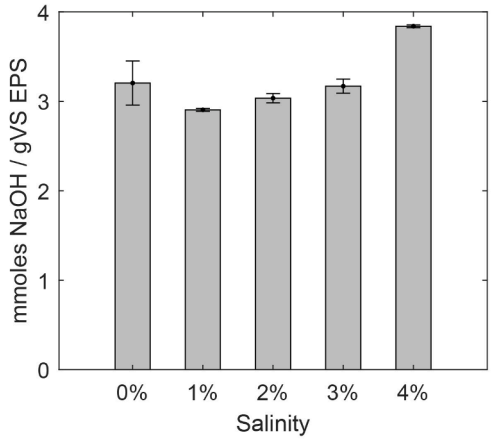

Fig. 6. Charge density of the EPS at different salinity concentrations as determined by conductometric titrations.

higher salinity, suggesting a higher productions of sulfated glycoproteins. Moreover, lectins binding sialic acid (*e.g.* PVL and rACG) displayed strong signal at $EPS_{4\%}$, consistent with the FT-IR analysis and sialic acid staining of the granules. The sialic acid-containing glycoprotein from the $EPS_{4\%}$ was further investigated by employing the MAA (MAL + MAH) lectin column for enrichment. The enriched glycoprotein contained sialic acids and GalNAcβ1–4GlcNAc (also known as LacDiNAc) based on the lectin microarray analysis (Fig. 5, indicated by the asterisk). After sialidase treatment, the signal of sialic acids lectins PVL and rACG significantly decreased by 7.5-fold and 1.5-fold, respectively (Supplementary Material Fig. S2), confirming both the presence of sialic acids, and the α(2 → 3) linkage between sialic acids and the penultimate sugar. As N-acetyl galactosamine is one possible penultimate sugar connected with sialic acids (de Graaff et al., 2019), there is a high probability that the structure Siaα2–3GalNAcβ1–4GlcNAc is present in the glycoprotein in $EPS_{4\%}$. Overall, the lectin microarray analysis provided a clear comparison among the glycan structure of glycoproteins in the extracted EPS, showing that with increasing salinity, although glycan diversity decreased, the charged groups (*e.g.* sialic acids, sulfates) and O-glycosylation became more prominent.

3.4. Charge density of the EPS

As glycoproteins with charged groups (sialic acids, sulfate groups) appeared to increase as a response to higher salinity, they may influence the total charge of the EPS and thereby on the AGS. To investigate the charge density of the extracted EPS, conductometric titrations were employed. The charge density of the EPS is expressed as the millimoles of NaOH per gram *VS* EPS (Fig. 6). Increasing salinity from 0 to 3% hardly caused a change in the charge density. However, under 4% salinity, the negative charge density of EPS increased by 19.8%, reaching 3.84 mmoles NaOH / gVS, in comparison to $EPS_{0\%}$. Compared to EPS of 1–3% salinity, this was increased by 32.3%, 26.5% and 21.1%, respectively. Probably, the increased amount of sialic acids of the glycoproteins, Probably, the increased amount of sialic acids of the glycoproteins, as observed with lectin microarray (Fig. 4) and lectin staining (Supplemental Material Fig. S1), is one of the contributing factors to the negative charge. These results indicate that $EPS_{4\%}$ was the most negatively charged.

3.5. Comparative metaproteomic analysis for microbial community and glycoconjugate - related proteins

3.5.1. Microbial community

The change in EPS properties, such as the charge and the glycan

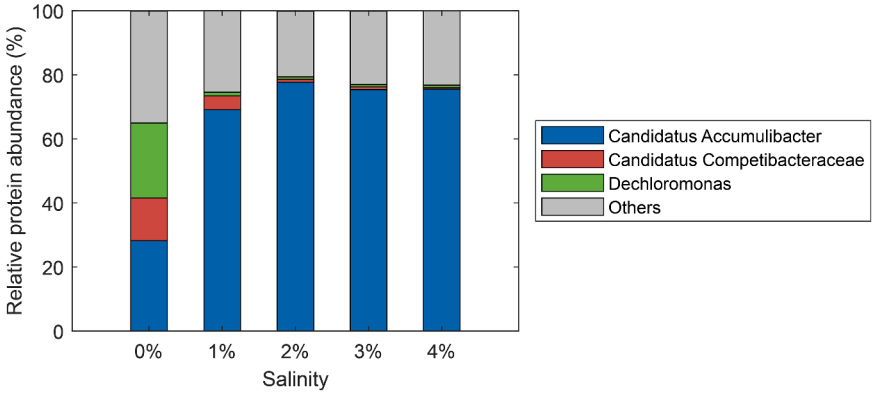

Fig. 7. Microbial community composition based on the number of identified peptides (peptide spectrum matches) assigned to the genus-level. Members making up less than <5 % of the total identified peptides are grouped in "Others".

profile in glycoproteins, raised the question: is this alteration connected with the shift of microbial community composition? To answer this question, metaproteomics was applied. In metaproteomics, all proteins in the microbial communities are studied (Kleikamp et al., 2023; Kleiner, 2019). Information obtained from these proteins can therefore not only be used to identify the composition of microbial communities, but also to investigate glycan production pathways and extracellular proteins.

Based on the metaproteomic analysis, the AGS microbial community was populated with a large fraction of phosphate accumulating organisms (PAO), such as "*Candidatus* Accumulibacter ("*Ca.* Accumulibacter") (Fig. 7). The abundance increased from 28% at 0% salinity to 69% at 1% salinity and remained constant at approximately 75% for the remainder of the salinities. Especially, based on the phylogenetic analysis of the PAO marker gene *ppk1* genes in the metagenome combined with the coverage depth data, it seems that only an unclassified Accumulibacter clade I species (closely related to GCA032229525.1) was dominant throughout the 1 to 4% salinity reactor runs, reaching 64% - 90% of the total *ppk1* genes coverage depth counts (Supplementary Material Fig. S3). Other bacteria, specifically Dechloromonas and glycogen accumulating organism (GAO) "*Candidatus* Competibacter", were only present in large amounts under the freshwater (0%) condition (23% and 13%, respectively), but both reduced to $< 5\%$ at $1 - 4\%$ salinity. Thus, the microbial community was more diverse under freshwater condition, while increasing salinity led to a stable microbial community with the dominance of a single "*Ca.* Accumulibacter" species. In this respect, it is reasonable to assume that the dominant "*Ca.* Accumulibacter" species is likely the main producer of the alternated EPS glycans in response to the increased salinity.

3.5.2. *Nucleotide sugars and glycoconjugates*

Regarding glycan synthesis, one of the prerequisite steps is activating the monosaccharide to a high-energy donor form called nucleotide sugar. These nucleotide sugars are monosaccharides linked to a mono-, di-, tri-nucleoside phosphates, such as uridine diphosphate (UDP), resulting in the activated sugar (Li et al., 2017; van Ede et al., 2025). Several enzymes such as kinases, epimerases, pyrophosphorylase, are involved in the formation of nucleotide sugars (Freeze and Elbein, 2022).

As "*Ca.* Accumulibacter", an assumed EPS producer (He and Mcmahon, 2011; Martinez, 2023), remained strongly present across the increased salinity range (1 - 4%), the metaproteomic analysis was therefore focused on this organism, which contributed the majority proteins associated with glycan synthesis. Metaproteomic analysis revealed 7 enzymes involved in the biosynthesis of nucleotide sugars that were significantly upregulated at 4% salinity, indicating a higher production of these nucleotide sugars (Red indicates a higher-than-average protein abundance and blue indicates a

Table 3
Upregulated proteins identified involved in the biosynthesis of nucleotide sugars with reported roles in glycans of "*Ca.* Accumulibacter" across all salinity concentrations based on KEGG. Representative protein names are shown; in some cases, multiple orthologous proteins perform the same function and are mapped to the same KO number based on the KEGG database (Supplementary Materials Table S2).

Proteins upregulated	Enzyme activity	Nucleotide sugar donors	Reported glycoconjugate	Reference
RfbA	TDP-Glc pyrophosphorylase	dTDP-Glc	O-antigen of LPS	Samuel & Reeves (2003)
WecB	UDP-GlcNAc epimerase	UDP-ManNAc	O-antigen of LPS	Samuel & Reeves (2003)
WlbA	UDP-GlcNAcA dehydrogenase	UDP-3-keto-GlcNAcA	O-antigen of LPS	Thoden & Holden (2011)
GmhA	Sedoheptulose-7-phosphate isomerase	D-glycero- β -D-manno-Heptose 7-phosphate	LPS (core and/or O-antigen), CP	Valvano et al. (2002)
GmhD	ADP-D-glycero-β-D-manHep epimerase	ADP-L-glycero- β -D-manno-heptose	LPS (core and/or O-antigen), CP	Valvano et al. (2002)
GlmU	GlcNAc-1P pyrophosphorylase	UDP-GlcNAc	Many glycans	Tytgat & Lebeer (2014)
GalE	UDP-Glc epimerase	UDP-Gal	Many glycans	Tytgat & Lebeer (2014)

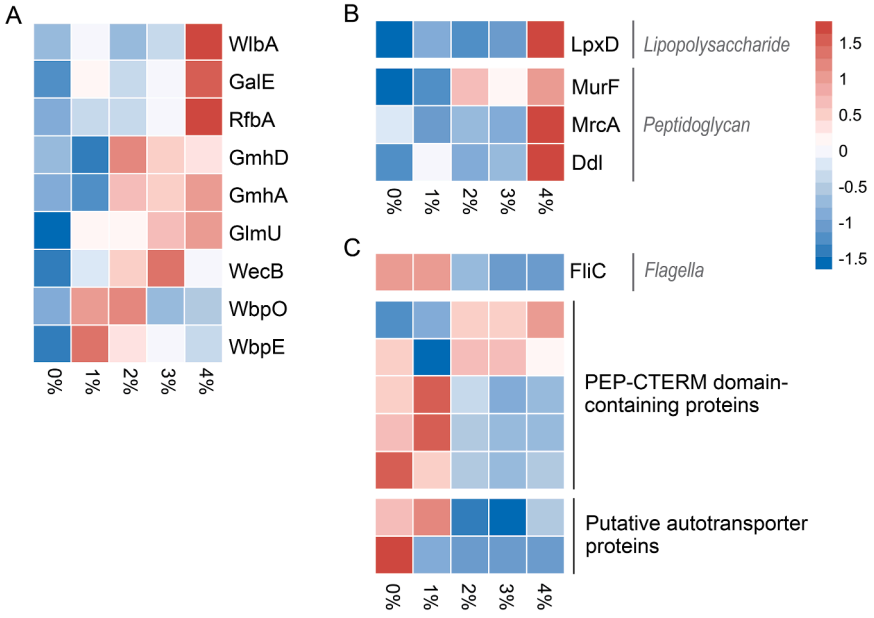

Fig. 8. Comparative analysis of the proteins of "*Ca.* Accumulibacter" genus closely involved in the biosynthesis of nucleotide sugars (A) and glycoconjugates responding to salinity (B and C). The glycoconjugates are divided into proteins involved in pathways for the biosynthesis of lipopolysaccharides and peptidoglycans (B) and putative glycoproteins based on the KEGG database and database (NCBI / Uniprot) annotations (C). Proteins with no direct link to the production of glycans are excluded in this figure (*i.e.* proteins part of the glycolysis). Red indicates a higher-than-average protein abundance and blue indicates a lower-than-average protein abundance.

Table 4
Downregulated proteins identified involved in the biosynthesis of nucleotide sugars with reported roles in glycans of "*Ca.Accumulibacter*" across all salinity concentrations based on KEGG. Representative protein names are shown; in some cases, multiple orthologous proteins perform the same function and are mapped to the same KO number (Supplementary Table S2).

Proteins downregulated	Enzyme activity	Sugar product	Reported function	Reference
WbpO	UDP-GlcNAc dehydrogenase	UDP-GalNAcA / UDP-GlcNAcA	Extracellular PS	Li et al. (2016)
WbpE	UPD-3-keto-GlcNAcA aminotransferase	UDP-GlcNAc3NA	O-antigen of LPS	Thoden & Holden (2011)

lower-than-average protein abundance Table 3, Fig. 8A). Two enzymes were upregulated followed by a downregulation (Table 4, Fig. 8A). Among these upregulated nucleotide sugars, dTDP-Glu, UDP-ManNAc, UDP-3-keto-GlcNAcA and ADP-L-glycero-β-D-manno-heptose are reported as important glycosylation precursors in the synthesis of lipopolysaccharides. Only UDP-GlcNAc and UDP-Gal are essential precursors in various glycans, *i.e.* UDP-GlcNAc could be involved in protein glycosylation by O-GlcNAcylation, incorporated in cell wall structures, or used as a precursor for sialic acid synthesis (Chatham and Marchase, 2010; Han et al., 2019; Varki and Schauer, 2009). UDP-Gal could be incorporated as a residue in the glycoprotein glycan or used as a precursor for the synthesis of exopolysaccharides (Tytgat and Lebeer, 2014).

Thus, among the detected enzymes that are involved in the biosynthesis of nucleotide sugars precursors, those potentially lead to the synthesis of LPS were found strongly upregulated at higher salinity. This pointed to the production of more LPS as a response to increasing salinity. In fact, when the enzymes involved along the pathways of LPS and other cell wall glycans synthesis were searched in the metaproteomic results, a few enzymes were indeed found upregulated (Fig. 8B), *i.e.* LpxD, which is responsible for catalyzing the third step in lipid A biosynthesis (Bertani and Ruiz, 2018), and three enzymes (MurF, Ddl, MrcA) related to peptidoglycan synthesis (MurF and Ddl) are involved in the stepwise assembly of the peptide stem of peptidoglycan and MrcA is a peptidoglycan transferase that catalyzes one of the last steps in the biosynthesis of peptidoglycan (Barreteau et al., 2008). Unfortunately, enzymes directly related to known protein glycosylation pathways, such as the *en bloc* pathways (Li et al., 2017; Nothaft and Szymanski, 2010), were not detected.

3.6. Response of putative glycoproteins to the increasing salinity

The lectin microarray analysis confirmed the presence of glycoproteins, while the enzymes related to known protein glycosylation pathways were hardly observed in the metaproteomic data. Therefore, potential glycosylated protein candidates were searched in the metaproteome based on the annotations in literature (Li et al., 2017; Nothaft and Szymanski, 2010; Olst et al., 2025; Tytgat and Lebeer, 2014) (Fig. 8C). Several putative glycoproteins were identified in the metaproteome for "*Ca.* Accumulibacter", including FliC, the flagellin filament of flagella, PEP-CTERM domain-containing proteins, and bacterial autotransporters. FliC was detected consistently but significantly downregulated at higher salinity. Among the five annotated PEP-CTERM proteins, three were downregulated and two upregulated. Two putative autotransporter proteins were detected and both showed a decrease in abundance with increasing salinity. Potential glycosylation sites reveal high % of potential O- and N-glycosylation for FliC (9.3%), followed by the bacterial autotransporter (6.5%, 1.8%, respective to Fig. 8C) and PEP-CTERM proteins (1.0 – 2.0%) (Supplementary Material Table S3). Apparently, most of these putative glycoproteins which were reported related to biofilm formation were downregulated. To summarize, the LPS and peptidoglycan biosynthesis appear to be upregulated with increasing salinity. Several putative glycoproteins were detected to be downregulated with increasing salinity.

4. Discussion

4.1. Adaptive response of extracellular polymeric substances of aerobic granular sludge on the increasing salinity

Previous works on saline AGS have shown contradictory responses in the EPS towards salinity; increased protein (Campo et al., 2018; Ou et al., 2018) and polysaccharide contents have been observed (Hou et al., 2019). However, in these cases it remains unclear whether the changes observed are due to gradual aging of the biomass or actual adaptation of the microorganisms in the EPS. Moreover, conventional EPS characterization metrics, such as the PN/PS ratio, are insufficient to fully characterize the changes within the EPS (Felz et al., 2019). To address these limitations, in this work it was ensured that at least 90% of the biomass was renewed prior to EPS analysis, thereby capturing microbial adaptations rather than aging effects. Importantly, EPS glycoconjugate characterization was performed in combination with metaproteomics, allowing us to connect the glycan specific modifications and charge density changes to a single "*Ca.* Accumulibacter" clade. This approach provides a more detailed understanding of EPS responses AGS under salinity stress.

The seawater salinity in a lab-scale aerobic granular sludge (AGS) reactor was stepwise increased, starting from freshwater condition (0% salinity), reaching up to 4% salinity with 1%pt. increments, to investigate the microbial and extracellular polymeric substances (EPS) adaptations. Initially, at 0% salinity, the microbial community was diverse, besides "*Ca.* Accumulibacter" (28%), there were Dechloromonas (23%) and "*Ca.* Competibacter" (13%) present. As the salinity increased to 1 %, the community shifted to one dominant "*Ca.* Accumulibacter" species (69% – 75%) and remained similar until 4% salinity. Regarding the chemical composition of the granules, carbohydrate-related functional groups first increased by 0% and decreased when the salinity was increased. While sialic acid content followed the opposite trend. These shifts were reflected in the glycoproteins of the EPS: lectin microarray indicated a reduction in glycan diversity, along with an increase of charged groups such as sialic acids and sulfated groups. The overall negative charge of the total EPS was found to increase at higher salinity, corresponding to the increase of these charged groups. Thus, despite the stable granule morphology and dominance of a single species of "*Ca.* Accumulibacter" between 1% and 4% seawater salinity, significant changes in the EPS were observed. These findings indicated that the same microorganisms adjusted their EPS composition, as a response to increased salinity, particularly by modifying the glycoproteins with more negatively charged groups.

The increased negative charge in the EPS might be explained by the Derjaguin–Landau–Verwey–Overbeek (DLVO) theory of colloidal stability (Hermansson, 1999). According to this theory, when salinity increases, the range of the repulsive forces between the negatively charged functional groups decreases. This can cause unwanted aggregation of particles, such as proteins, leading to a loss in stability and/or function. To overcome this, microorganisms may produce EPS carrying more negatively charged groups, due to the fact that charged groups could facilitate electrostatic interactions or hydrogen bonding, creating a protein-water-salt hydration matrix. This leads to reduced protein aggregation and increased flexibility, so that the functions of proteins can still be maintained (Gunde-Cimerman et al., 2018; Howard et al., 2009; Zaccai et al., 1989). Microorganisms can adopt different strategies to

enhance the negative charge of their proteins. Halophilic Archaea produce a highly acidic proteome when they are exposed to salinity (Gunde-Cimerman et al., 2018). Their proteins have a significant excess of negatively charged amino acids over amino acids with a positive charge. In the S-layer glycoprotein from the extreme halophile *Halobacterium halobium*, sulfated glucuronic acid residues are in the glycans of this glycoprotein, causing a drastic increase in surface charge density (Mengele and Sumper, 1992).

In the current research, another strategy for increased charges was highlighted: microorganisms in AGS produce/modify the glycoproteins with more sialic acids and sulfated groups to increase the negative charge of the proteins. Sulfated groups, the most charged glycan modification known to exist, are found along the glycan chain, whereas sialic acids, which are nine-carbon sugars, are typically found at the terminal ends of glycans (de Graaff et al., 2019; Mengele and Sumper, 1992; Varki et al., 2017b). Both modifications are reported to exhibit functions through their charge, such as hydration (Varki et al., 2017b), protein binding (Bedini et al., 2019) and gel-formation through Ca^{2+} mediated cross-links (Meldrum et al., 2018). Collectively, these functions may contribute to structural stabilization in the EPS matrix at increased salinities. Although in previous work it was found that sialic acids and sulfated groups are widely spread in granular sludge (Boleij et al., 2020; Chen et al., 2023a; Felz et al., 2019), this research demonstrates that decorating the glycans of glycoproteins with sialic acids and sulfated groups may represent an adaptive strategy of "*Ca.* Accumulibacter" under saline conditions. It supports the hypothesis from our earlier study (Chen et al., 2024) that AGS microorganisms actively produce more charged EPS as a response to increased salinity, maintaining protein function, granule integrity, and stability and thereby supporting the structural resilience of the granules under stress conditions.

4.2. Exploring protein glycosylation pathways and the possible glycoprotein candidates through metaproteomics

Metaproteomics enables the study of biosynthesis pathways by identifying specific enzymes (Kleiner, 2019). Despite the finding of both N- and O-linked glycoproteins by lectin microarray, the enzymes involved in known glycosylation pathways have not been found at all, despite the potential reported earlier (Páez-Watson et al., 2024). Instead, enzymes related to LPS and peptidoglycans were found, with a clear upregulation tendency with salinity. This could be explained by a few reasons. Firstly, there is considerable overlap between glycosylation pathways, especially the LPS and glycoprotein glycan assembly pathways share diverse transferases and transporters (Hug and Feldman, 2011). Secondly, some nucleotide sugars may be shared by different glycoconjugate pathways. For example, UDP-GlcNAc is utilized in the synthesis of peptidoglycans, LPS and glycoproteins (Li et al., 2017). Moreover, some enzymes may have functions in different glycoconjugate biosynthesis pathways, *e.g.* glycosyltransferases, which catalyze the transfer of nucleotide sugar on a molecule, can sometimes participate in more than one pathway. In *Acinetobacter baumannii,* for example, the same glycosyltransferase participates in the synthesis of both glycoproteins and capsule polysaccharides (Lees-Miller et al., 2013). As glycan synthesis is non-template driven and complex, it is still challenging to find the exact protein glycosylation pathways by only searching for upregulated or downregulated enzymes in the metaproteome. Nevertheless, it is uncertain which pathways are responsible for the synthesis of the glycoprotein glycans in *"Ca.* Accumulibacter", but with the current evidence, it can be suggested that these pathways may share components with the LPS biosynthesis pathway (Hug and Feldman, 2011; Szymanski, 2022).

An alternative strategy is to screen for the known glycoproteins reported in the literature in the metaproteome. It revealed the presence of potential O-linked glycoprotein candidates: flagella, PEP-CTERM proteins, and bacterial autotransporters, which have been described to be involved in biofilm-related functions. While flagella are typically associated with initial surface attachment (Guttenplan and Kearns, 2013), they may also play a role in EPS matrix stabilization (Flemming and Wingender, 2010). Their detection in this study is notable, especially since they have not been observed for "*Ca.* Accumulibacter" before, despite the presence of the biosynthesis genes (Martín et al., 2006) and its expression on the metatranscriptome (Kondrotaite et al., 2025). This suggests a potential overlooked function of the flagella protein produced by "*Ca.* Accumulibacter". PEP-CTERM proteins, recently identified as an abundant protein in a "*Ca.* Accumulibacter" culture (Olst et al., 2025), are rich in amino acids serine (Ser), threonine (Thr) and asparagine (Asn). Ser and Thr are the amino acids most commonly glycosylated in O-glycosylation, while Asn is the most common site for N-glycosylation (Haft et al., 2006; Kelly et al., 2022). These proteins have been associated with floc formation in *Zoogloea* (Gao et al., 2018). Bacterial autotransporters, a class of outer membrane proteins, possess several functions, including bacterial adhesion and cell-to-cell aggregation (Tytgat and Lebeer, 2014; Wells et al., 2007). Although lectin microarray indicated an increased signal of glycan motifs commonly associated with O-linked glycoproteins with increasing salinity, metaproteomic data demonstrated the downregulation of flagella, PEP-CTERM protein, and bacterial autotransporters. This discrepancy is likely a reflection of the following reasons: The knowledge of bacterial glycoproteins is limited and largely based on the pathogenic model organisms, such as *Campylobacter jejuni* (Li et al., 2017; Szymanski, 2022), leaving many glycoproteins undiscovered. Thus, the three proteins above are "a small piece of an iceberg" in the glycoproteins in AGS; their change cannot represent the change of the total O-linked glycoproteins shown by the lectin microarray. On the other hand, their downregulation at higher salinity seems logical. If higher salinity may already cause aggregation of particles due decreased electrostatic repulsion, as a counter reaction, microorganisms produce EPS carrying more negatively charged groups. It is not necessary to spend energy to produce those aggregation-related glycoproteins.

4.3. Advancing the development of methodologies in the EPS research

These findings have practical implications for both the operation of AGS systems and resource recovery. Despite maintaining the same granule morphology, the EPS is clearly adapted at the microscale. Those EPS adaptations in the glycoconjugates suggest that microbial community can maintain granule stability and performance under elevated salinity. These changes in the EPS charge and glycoproteins composition could serve as an indicator of microbial adaptation and guide operational adjustments, particularly under saline conditions. Besides, the EPS adaptations observed in this work highlight the need for more analytical approaches to gain better understanding of the EPS. With the rapid development of omics techniques, it is important to implement these tools in EPS research. It is known that bacteria can synthesize a diverse array of glycans, being attached to proteins and lipids, or as loosely associated polysaccharides to the cells. Through metagenomics, it is possible to identify the dominance of a single species of "*Ca.* Accumulibacter" in the microbial community. Glycomics, on the other hand, is the comprehensive study of glycans, it helps understand the role of glycans in bacterial cell-cell and cell–environment interactions (Rudd et al., 2022). Furthermore, metaproteomics is the study of all proteins in microbial communities (Kleiner, 2019). Information obtained can be used to identify the composition of microbial communities, the enzymes related to metabolic pathways, and the extracellular proteins. In the current research, the high-throughput lectin microarray enables monitoring changes in glycosylation patterns of glycoproteins under various salinity conditions. It also provides insights into glycosidic linkages and helps establish correlations between salinity and protein glycosylation in the EPS. Probably, these two omics tools, glycomics and metaproteomics (Pabst et al., 2022), need to be added to the multidisciplinary roadmap for resolving the EPS composition and function

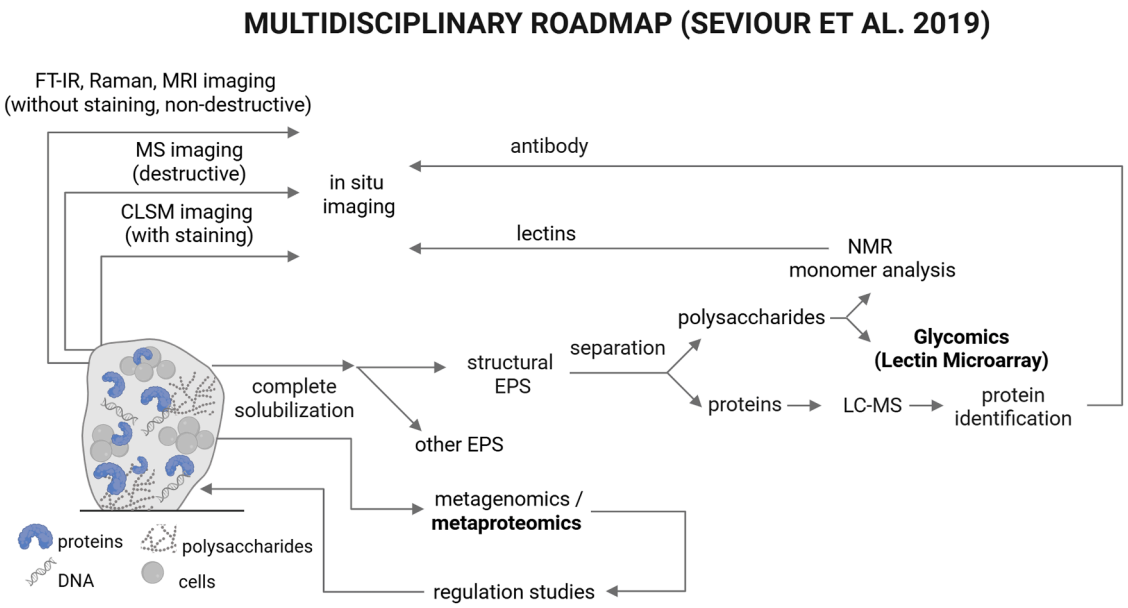

Fig. 9. Multidisciplinary roadmap for resolving the EPS function and identity as proposed by Seviour et al. (2019). Metaproteomic and lectin microarray are included, expanding the roadmap.

proposed by Seviour et al., (2019) (Fig. 9).

It is worth noting that, although both lectin microarray and metaproteomics revealed significant new insights in the EPS adaptation to the increasing salinities, a few challenges remain: For the lectin microarray, the limitations mainly lie in the structural epitopes that are recognized by the lectins and their commercial availability (Poole et al., 2018). No lectins reflecting bacterial-specific glycan structures are available. Limitations of metaproteomics, on the other hand, arise from protein functional annotations (Heyer et al., 2017; Kleikamp et al., 2023). The information obtained is limited to the known pathways. This makes it challenging to connect the metabolic pathways with the specific glycan output, especially in a diverse microbial community such as the granular sludge in this research. Additionally, many glycosylation-related enzymes function across multiple glycoconjugate pathways and thus may be overlooked during the analysis. Therefore, detailed structural characterization of glycoconjugates is essential for understanding their biosynthetic pathways and roles within the EPS (Szymanski, 2022).

5. Conclusions

- Glycan diversity on glycoproteins decreases with increasing salinity, while the negatively charged groups, sialic acids and sulfated groups, increased.
- The increase in salinity resulted to a shift from a more diverse microbial community to a dominant community of "*Ca.* Accumulibacter".
- Increasing the negative charge in the EPS, specifically the glycoproteins, is an adaptive response towards increasing salinity by "*Ca.* Accumulibacter".
- Increased salinity induced upregulation of various glycoconjugates, including LPS and peptidoglycans.
- Flagella, bacterial autotransporters, and PEP-CTERM domain-containing proteins were identified in the AGS as putative glycoproteins using metaproteomics.

Declaration of generative AI and AI-assisted technologies in the writing process

During the preparation of this work the author(s) used ChatGPT GPT-4o in order to improve the readability and structure. After using this tool/service, the author(s) reviewed and edited the content as needed and take(s) full responsibility for the content of the publication.

CRediT authorship contribution statement

Le Min Chen: Writing – review & editing, Writing – original draft, Investigation, Data curation. **Sunanda Keisham:** Writing – review & editing, Formal analysis, Data curation. **Hiroaki Tateno:** Writing – review & editing, Methodology, Investigation. **Gijs Y. Kleine:** Writing – review & editing, Methodology, Formal analysis, Data curation. **Martin Pabst:** Writing – review & editing, Formal analysis, Data curation. **Mario Pronk:** Writing – review & editing, Supervision, Methodology, Conceptualization. **Mark C.M. van Loosdrecht:** Writing – review & editing, Supervision, Conceptualization. **Yuemei Lin:** Writing – review & editing, Writing – original draft, Supervision, Investigation, Data curation, Conceptualization.

Declaration of competing interest

The authors declare that they have no known competing financial interests or personal relationships that could have appeared to influence the work reported in this paper.

Acknowledgments

The authors acknowledge Siem van Eerden for the support for identifying the "*Ca.* Accumulibacter" species based on the metagenomic dataset. This research was financially supported by TKI Chemie 2017 (co-funded by Haskoning), from the Dutch Ministry of Economic Affairs and Climate Policy.

Supplementary materials

Supplementary material associated with this article can be found, in the online version, at doi:10.1016/j.watres.2025.125313.

Data availability

Data will be made available on request.

References

Andrews, S., 2010. FastQC: a quality control analysis tool for high throughput sequencing data [WWW Document]. URL https://github.com/s-andrews/FastQC?tab=readme-ov-file#readme (accessed 7.14.25).

APHA, 1998. Standard Methods For the Examination of Water and Wastewater, 20th ed. American Public Health Association, American Water Works Association, Water Environment Federation, Washington, D.C. 1998.

Barreteau, H., Kovač, A., Boniface, A., Sova, M., Gobec, S., Blanot, D., 2008. Cytoplasmic steps of peptidoglycan biosynthesis. FEMS Microbiol. Rev. 32, 168–207. https://doi.org/10.1111/J.1574-6976.2008.00104.X.

Bedini, E., Corsaro, M.M., Fernández-Mayoralas, A., Iadonisi, A., 2019. Chondroitin, dermatan, heparan, and keratan sulfate. Struct. Funct. 187–233. https://doi.org/10.1007/978-3-030-12919-4_5.

Bertani, B., Ruiz, N., 2018. Function and biogenesis of lipopolysaccharides. EcoSal. Plus. 8. https://doi.org/10.1128/ECOSALPLUS.ESP-0001-2018.

Boleij, M., Kleikamp, H., Pabst, M., Neu, T.R., van Loosdrecht, M.C.M., Lin, Y., 2020. Decorating the Anammox House: sialic acids and sulfated glycosaminoglycans in the extracellular polymeric substances of anammox granular sludge. Environ Sci Technol ACS.EST. https://doi.org/10.1021/acs.est.9b07207, 9b07207.

Breitwieser, F.P., Salzberg, S.L., 2020. Pavian: interactive analysis of metagenomics data for microbiome studies and pathogen identification. Bioinformatics 36, 1303–1304. https://doi.org/10.1093/BIOINFORMATICS/BTZ715.

Campo, R., Corsino, S.F., Torregrossa, M., Di Bella, G., 2018. The role of extracellular polymeric substances on aerobic granulation with stepwise increase of salinity. Sep. Purif. Technol. 195, 12–20. https://doi.org/10.1016/j.seppur.2017.11.074.

Chatham, J.C., Marchase, R.B., 2010. Protein O-GlcNAcylation: a critical regulator of the cellular response to stress. Curr. Signal. Transduct. Ther. 5, 49. https://doi.org/10.2174/157436210790226492.

Chen, L.M., Beck, P., van Ede, J., Pronk, M., van Loosdrecht, M.C.M., Lin, Y., 2024. Anionic extracellular polymeric substances extracted from seawater-adapted aerobic granular sludge. Appl. Microbiol. Biotechnol. 108, 144. https://doi.org/10.1007/s00253-023-12954-x.

Chen, L.M., de Bruin, S., Pronk, M., Sousa, D.Z., van Loosdrecht, M.C.M., Lin, Y., 2023a. Sialylation and sulfation of anionic glycoconjugates are common in the extracellular polymeric substances of both aerobic and Anaerobic granular sludges. Environ. Sci. Technol. 57, 13217–13225. https://doi.org/10.1021/acs.est.2c09586.

Chen, L.M., Keisham, S., Tateno, H., Ede, J.V., Pronk, M., Loosdrecht, M.C.M.V., Lin, Y., 2023b. Alterations of glycan composition in aerobic granular sludge during the adaptation to seawater conditions. ACS ES&T Water. https://doi.org/10.1021/ACSESTWATER.3C00625.

Chen, S., 2023. Ultrafast one-pass FASTQ data preprocessing, quality control, and deduplication using fastp. Imeta 2, e107. https://doi.org/10.1002/IMT2.107;JOURNAL:JOURNAL:2770596X.

Corsino, S.F., Capodici, M., Torregrossa, M., Viviani, G., 2017. Physical properties and extracellular Polymeric substances pattern of aerobic granular sludge treating hypersaline wastewater. Bioresour. Technol. 229, 152–159. https://doi.org/10.1016/j.biortech.2017.01.024.

de Graaff, D.R., Felz, S., Neu, T.R., Pronk, M., van Loosdrecht, M.C.M., Lin, Y., 2019. Sialic acids in the extracellular polymeric substances of seawater-adapted aerobic granular sludge. Water. Res. 343–351. https://doi.org/10.1016/j.watres.2019.02.040.

de Graaff, D.R., van Loosdrecht, M.C.M., Pronk, M., 2020. Biological phosphorus removal in seawater-adapted aerobic granular sludge. Water. Res. 172, 115531. https://doi.org/10.1016/J.WATRES.2020.115531.

Eichler, J., Koomey, M., 2017. Sweet new roles for protein glycosylation in prokaryotes. Trends. Microbiol. 25, 662–672. https://doi.org/10.1016/J.TIM.2017.03.001.

Felz, S., Vermeulen, P., van Loosdrecht, M.C.M., Lin, Y.M., 2019. Chemical characterization methods for the analysis of structural extracellular polymeric substances (EPS). Water. Res. 157, 201–208. https://doi.org/10.1016/j.watres.2019.03.068.

Flemming, H.C., Wingender, J., 2010. The biofilm matrix. Nat. Rev. Microbiol. https://doi.org/10.1038/nrmicro2415.

Freeze, H.H., Elbein, A.D., 2022. Glycosylation precursors. Essentials of Glycobiology [Internet], 4th Edition. Cold Spring Harbor Laboratory Press.

Gao, N., Xia, M., Dai, J., Yu, D., An, W., Li, S., Liu, S., He, P., Zhang, L., Wu, Z., Bi, X., Chen, S., Haft, D.H., Qiu, D., 2018. Both widespread PEP-CTERM proteins and exopolysaccharides are required for floc formation of Zoogloea resiniphila and other activated sludge bacteria. Environ. Microbiol. 20, 1677–1692. https://doi.org/10.1111/1462-2920.14080.

Gunde-Cimerman, N., Plemenitaš, A., Oren, A., 2018. Strategies of adaptation of microorganisms of the three domains of life to high salt concentrations. FEMS Microbiol. Rev. 42, 353–375. https://doi.org/10.1093/femsre/fuy009.

Guttenplan, S.B., Kearns, D.B., 2013. Regulation of flagellar motility during biofilm formation. FEMS Microbiol. Rev. 37, 849–871. https://doi.org/10.1111/1574-6976.12018.

Haft, D.H., Paulsen, I.T., Ward, N., Selengut, J.D., 2006. Exopolysaccharide-associated protein sorting in environmental organisms: the PEP-CTERM/SpsH system. Application of a novel phylogenetic profiling heuristic. BMC. Biol. 4, 1–16. https://doi.org/10.1186/1741-7007-4-29/TABLES/4.

Han, H., Song, B., Joon Song, M., Yoon, S., 2019. Enhanced nitrous oxide production in denitrifying dechloromonas aromatica strain RCB under salt or alkaline stress conditions. Front. Microbiol. 10. https://doi.org/10.3389/FMICB.2019.01203.

He, S., Mcmahon, K.D., 2011. Microbiology of "Candidatus Accumulibacter" in activated sludge. Microb. Biotechnol. https://doi.org/10.1111/j.1751-7915.2011.00248.x.

Hermansson, M., 1999. The DLVO theory in microbial adhesion. Colloids. Surf. B Biointerfaces. 14, 105–119. https://doi.org/10.1016/S0927-7765(99)00029-6.

Heyer, R., Schallert, K., Zoun, R., Becher, B., Saake, G., Benndorf, D., 2017. Challenges and perspectives of metaproteomic data analysis. J. Biotechnol. 261, 24–36. https://doi.org/10.1016/J.JBIOTEC.2017.06.1201.

Hou, M., Li, W., Li, H., Li, C., Wu, X., Liu, Y.D., 2019. Performance and bacterial characteristics of aerobic granular sludge in response to alternating salinity. Int. Biodeterior. Biodegradation. 142, 211–217. https://doi.org/10.1016/j.ibiod.2019.05.007.

Howard, S.L., Jagannathan, A., Soo, E.C., Hui, J.P.M., Aubry, A.J., Ahmed, I., Karlyshev, A., Kelly, J.F., Jones, M.A., Stevens, M.P., Logan, S.M., Wren, B.W., 2009. Campylobacter jejuni glycosylation island important in cell charge, legionaminic acid biosynthesis, and colonization of chickens. Infect. Immun. 77, 2544–2556. https://doi.org/10.1128/IAI.01425-08/ASSET/2C99F5B4-D3AB-409E-8DDA-545A901E7DBB/ASSETS/GRAPHIC/ZII0060979990007.JPEG.

Hug, I., Feldman, M.F., 2011. Analogies and homologies in lipopolysaccharide and glycoprotein biosynthesis in bacteria. Glycobiology 21, 138–151. https://doi.org/10.1093/GLYCOB/CWQ148.

Kaminski, L., Guan, Z., Yurist-Doutsch, S., Eichler, J., 2013. Two distinct N-glycosylation pathways process the haloferax volcanii S-layer glycoprotein upon changes in environmental salinity. mBio 4. https://doi.org/10.1128/MBIO.00716-13.

Kang, D.D., Li, F., Kirton, E., Thomas, A., Egan, R., An, H., Wang, Z., 2019. MetaBAT 2: an adaptive binning algorithm for robust and efficient genome reconstruction from metagenome assemblies. PeerJ. 2019, e7359. https://doi.org/10.7717/PEERJ.7359/SUPP-3.

Kelly, J., Vinogradov, E., Robotham, A., Tessier, L., Logan, S.M., Jarrell, K.F., 2022. Characterizing the N- and O-linked glycans of the PGF-CTERM sorting domain-containing S-layer protein of Methanoculleus marisnigri. Glycobiology 32, 629–644. https://doi.org/10.1093/GLYCOB/CWAC019.

Kleikamp, H.B.C., Grouzdev, D., Schaasberg, P., van Valderen, R., van der Zwaan, R., Wijgaart, R.V.D., Lin, Y., Abbas, B., Pronk, M., van Loosdrecht, M.C.M., Pabst, M., 2023. Metaproteomics, metagenomics and 16S rRNA sequencing provide different perspectives on the aerobic granular sludge microbiome. Water. Res. 246, 120700. https://doi.org/10.1016/J.WATRES.2023.120700.

Kleine, G.Y., Wilfert, P.K., Picken, S.J., 2025. Quantifying charge density in complex biopolymer systems via conductometric titration. ACS. Omega. https://doi.org/10.1021/ACSOMEGA.5C07186.

Kleiner, M., 2019. Metaproteomics: much more than measuring gene expression in microbial communities. mSystems. 4. https://doi.org/10.1128/MSYSTEMS.00115-19/ASSET/AD6943B7-5C75-4ABB-8897-F622F004750A/ASSETS/GRAPHIC/MSYSTEMS.00115-19-F0001.JPEG.

Kondrotaite, Z., Petersen, J., Singleton, C., Peces, M., Petriglieri, F., Jensen, T.B.N., Sereika, M., Daugberg, A.O.H., Wagner, M., Dueholm, M.K.D., Nielsen, P.H., Rodrigues, J.L.M., 2025. Ecophysiology and niche differentiation of three genera of polyphosphate-accumulating bacteria in a full-scale wastewater treatment plant. mSystems. https://doi.org/10.1128/MSYSTEMS.00322-25.

Lees-Miller, R.G., Iwashkiw, J.A., Scott, N.E., Seper, A., Vinogradov, E., Schild, S., Feldman, M.F., 2013. A common pathway for O-linked protein-glycosylation and synthesis of capsule in Acinetobacter baumannii. Mol. Microbiol. 89, 816–830. https://doi.org/10.1111/MMI.12300/SUPPINFO.

Lefebvre, O., Moletta, R., 2006. Treatment of organic pollution in industrial saline wastewater: a literature review. Water. Res. 40, 3671–3682. https://doi.org/10.1016/J.WATRES.2006.08.027.

Li, H., Debowski, A.W., Liao, T., Tang, H., Nilsson, H.O., Marshall, B.J., Stubbs, K.A., Benghezal, M., 2017. Understanding protein glycosylation pathways in bacteria. Future Microbiol. 12, 59–72. https://doi.org/10.2217/FMB-2016-0166.

Li, Z., Hwang, S., Bar-Peled, M., 2016. Discovery of a unique extracellular polysaccharide in members of the pathogenic Bacillus that can Co-form with spores. J. Biol. Chem. 291, 19051–19067. https://doi.org/10.1074/JBC.M116.724708.

Martín, H.G., Ivanova, N., Kunin, V., Warnecke, F., Barry, K.W., McHardy, A.C., Yeates, C., He, S., Salamov, A.A., Szeto, E., Dalin, E., Putnam, N.H., Shapiro, H.J., Pangilinan, J.L., Rigoutsos, I., Kyrpides, N.C., Blackall, L.L., McMahon, K.D., Hugenholtz, P., 2006. Metagenomic analysis of two enhanced biological phosphorus removal (EBPR) sludge communities. Nat. Biotechnol. 24, 1263–1269. https://doi.org/10.1038/nbt1247.

Martinez, S.T., 2023. Extracellular Polymeric substances of "Candidatus Accumulibacter": composition, application and turnover. https://doi.org/10.4233/UUID:88CE92A5-153E-47E4-BB21-999237161AB7.

Meldrum, O.W., Yakubov, G.E., Bonilla, M.R., Deshmukh, O., McGuckin, M.A., Gidley, M.J., 2018. Mucin gel assembly is controlled by a collective action of non-mucin proteins, disulfide bridges, Ca2+ -mediated links, and hydrogen bonding. Sci. Rep. 8, 1–16. https://doi.org/10.1038/s41598-018-24223-3.

Mengele, R., Sumper, M., 1992. Drastic differences in glycosylation of related S-layer glycoproteins from moderate and extreme halophiles. J. Biol. Chem. 267, 8182–8185. https://doi.org/10.1016/S0021-9258(18)42424-6.

Nothaft, H., Szymanski, C.M., 2010. Protein glycosylation in bacteria: sweeter than ever. Nat. Rev. Microbiol. 11 (8), 765–778. https://doi.org/10.1038/nrmicro2383, 2010 8.

Nurk, S., Meleshko, D., Korobeynikov, A., Pevzner, P.A., 2017. MetaSPAdes: a new versatile metagenomic assembler. Genome Res. 27, 824–834. https://doi.org/10.1101/GR.213959.116/-/DC1.

Olst, B.V., Eerden, S.A., Eštok, N.A., Roy, S., Abbas, B., Lin, Y., Loosdrecht, M.C.M.V., Pabst, M., 2025. Metaproteomic profiling of the secretome of a granule-forming *Ca.* Accumulibacter Enrichment. Proteomics, e202400189. https://doi.org/10.1002/PMIC.202400189.

Ou, D., Li, W., Li, H., Wu, X., Li, C., Zhuge, Y., Liu, Y.D., 2018. Enhancement of the removal and settling performance for aerobic granular sludge under hypersaline stress. Chemosphere 212, 400–407. https://doi.org/10.1016/J.CHEMOSPHERE.2018.08.096.

Pabst, M., Grouzdev, D.S., Lawson, C.E., Kleikamp, H.B.C., de Ram, C., Louwen, R., Lin, Y.M., Lücker, S., van Loosdrecht, M.C.M., Laureni, M., 2022. A general approach to explore prokaryotic protein glycosylation reveals the unique surface layer modulation of an anammox bacterium. ISMe J. 16, 346–357. https://doi.org/10.1038/S41396-021-01073-Y.

Páez-Watson, T., Tomás-Martínez, S., de Wit, R., Keisham, S., Tateno, H., van Loosdrecht, M.C.M., Lin, Y., 2024. Sweet secrets: exploring novel glycans and glycoconjugates in the extracellular polymeric substances of "Candidatus Accumulibacter. ACS. ES. T. Water. 4, 3391–3399. https://doi.org/10.1021/ACSESTWATER.4C00247/ASSET/IMAGES/LARGE/EW4C00247_0005.JPEG.

Poole, J., Day, C.J., Von Itzstein, M., Paton, J.C., Jennings, M.P., 2018. Glycointeractions in bacterial pathogenesis. Nat. Rev. Microbiol. 7 (16), 440–452. https://doi.org/10.1038/s41579-018-0007-2, 2018 16.

Pronk, M., Bassin, J.P., De Kreuk, M.K., Kleerebezem, R., Van Loosdrecht, M.C.M., 2014. Evaluating the main and side effects of high salinity on aerobic granular sludge. Appl. Microbiol. Biotechnol. 98, 1339–1348. https://doi.org/10.1007/s00253-013-4912-z.

Pronk, M., de Kreuk, M.K., de Bruin, B., Kamminga, P., Kleerebezem, R., van Loosdrecht, M.C.M., 2015. Full scale performance of the aerobic granular sludge process for sewage treatment. Water. Res. 84, 207–217. https://doi.org/10.1016/j.watres.2015.07.011.

Rudd, P.M., Karlsson, N.G., Khoo, K.-H., Thaysen-Andersen, M., Wells, L., Packer, N.H., 2022. Glycomics and glycoproteomics. Essentials of glycobiology. https://doi.org/10.1101/GLYCOBIOLOGY.4E.51.

Samuel, G., Reeves, P., 2003. Biosynthesis of O-antigens: genes and pathways involved in nucleotide sugar precursor synthesis and O-antigen assembly. Carbohydr. Res. 338, 2503–2519. https://doi.org/10.1016/J.CARRES.2003.07.009.

Schäffer, C., Messner, P., 2017. Emerging facets of prokaryotic glycosylation. FEMS Microbiol. Rev. 41, 49. https://doi.org/10.1093/FEMSRE/FUW036.

Seemann, T., 2014. Prokka: rapid prokaryotic genome annotation. Bioinformatics. 30, 2068–2069. https://doi.org/10.1093/BIOINFORMATICS/BTU153.

Seviour, T., Derlon, N., Dueholm, M.S., Flemming, H.-C., Girbal-Neuhauser, E., Horn, H., Kjelleberg, S., van Loosdrecht, M.C.M., Lotti, T., Malpei, M.F., Nerenberg, R., Neu, T. R., Paul, E., Yu, H., Lin, Y., 2019. Extracellular polymeric substances of biofilms: suffering from an identity crisis. Water. Res. 151, 1–7. https://doi.org/10.1016/j.watres.2018.11.020.

Szymanski, C.M., 2022. Bacterial glycosylation, it's complicated. Front. Mol. Biosci. 9, 1015771. https://doi.org/10.3389/FMOLB.2022.1015771/BIBTEX.

Talari, A.C.S., Martinez, M.A.G., Movasaghi, Z., Rehman, S., Rehman, I.U., 2016. Advances in fourier transform infrared (FTIR) spectroscopy of biological tissues. 52, 456–506. https://doi.org/10.1080/05704928.2016.1230863.

Tateno, H., Toyota, M., Saito, S., Onuma, Y., Ito, Y., Hiemori, K., Fukumura, M., Matsushima, A., Nakanishi, M., Ohnuma, K., Akutsu, H., Umezawa, A., Horimoto, K., Hirabayashi, J., Asashima, M., 2011. Glycome diagnosis of human induced pluripotent stem cells using lectin microarray. J. Biol. Chem. 286, 20345–20353. https://doi.org/10.1074/jbc.M111.231274.

Thoden, J.B., Holden, H.M., 2011. Biochemical and structural characterization of WlbA from Bordetella pertussis and chromobacterium violaceum: enzymes required for the biosynthesis of 2,3-diacetamido-2,3-dideoxy- d -mannuronic acid. Biochemistry 50, 1483–1491. https://doi.org/10.1021/BI101871F/ASSET/IMAGES/LARGE/BI-2010-01871F_0007.JPEG.

Tytgat, H.L.P., Lebeer, S., 2014. The sweet tooth of bacteria: common themes in bacterial glycoconjugates. Microbiol. Mol. Biol. Rev. 78, 372. https://doi.org/10.1128/MMBR.00007-14.

Valvano, M.A., Messner, P., Kosma, P., 2002. Novel pathways for biosynthesis of nucleotide-activated glycero-manno-heptose precursors of bacterial glycoproteins and cell surface polysaccharides. Microbiology 148, 1979–1989. https://doi.org/10.1099/00221287-148-7-1979/CITE/REFWORKS.

van Ede, J.M., Soic, D., Pabst, M., 2025. Decoding sugars: mass spectrometric advances in the analysis of the sugar alphabet. Mass Spectrom. Rev. 1–52. https://doi.org/10.1002/MAS.21927;PAGE:STRING:ARTICLE/CHAPTER.

Varki, A., Cummings, R.D., Esko, J.D., Stanley, P., Hart, G.W., Aebi, M., Darvill, A.G., Kinoshita, T., Packer, N.H., Prestegard, J.H., Schnaar, R.L., Seeberger, P.H., 2017a. Essentials of Glycobiology. Cold Spring Harbor, NY, p. 823.

Varki, A., Schauer, R., 2009. Sialic Acids, chapter 14. Essentials Glycobiol. 9, 1–19.

Varki, A., Schnaar, R.L., Schauer, R., 2017b Sialic acids and other nonulosonic acids. https://doi.org/10.1101/GLYCOBIOLOGY.3E.015.

Vishniac, W., Santer, M., 1957. The thiobacilli. Bacteriol. Rev. 21, 195–213. https://doi.org/10.1128/BR.21.3.195-213.1957.

Wang, X., Yang, T., Lin, B., Tang, Y., 2017. Effects of salinity on the performance, microbial community, and functional proteins in an aerobic granular sludge system. Chemosphere 184, 1241–1249. https://doi.org/10.1016/j.chemosphere.2017.06.047.

Welles, L., Lopez-Vazquez, C.M., Hooijmans, C.M., Van Loosdrecht, M.C.M., Brdjanovic, D., 2014. Impact of salinity on the anaerobic metabolism of phosphate-accumulating organisms (PAO) and glycogen-accumulating organisms (GAO). Appl. Microbiol. Biotechnol. 98, 7609–7622. https://doi.org/10.1007/s00253-014-5778-4.

Wells, T.J., Tree, J.J., Ulett, G.C., Schembri, M.A., 2007. Autotransporter proteins: novel targets at the bacterial cell surface. FEMS Microbiol. Lett. 274, 163–172. https://doi.org/10.1111/J.1574-6968.2007.00833.X.

Wood, D.E., Lu, J., Langmead, B., 2019. Improved metagenomic analysis with Kraken 2. Genome Biol. 20, 1–13. https://doi.org/10.1186/S13059-019-1891-0/FIGURES/2.

Zaccai, G., Cendrin, F., Haik, Y., Borochov, N., Eisenberg, H., 1989. Stabilization of halophilic malate dehydrogenase. J. Mol. Biol. 208, 491–500.

Zhang, Z., Sato, Y., Dai, J., Chui, H.K., Daigger, G., Van Loosdrecht, M.C.M., Chen, G., 2023. Flushing toilets and cooling spaces with seawater improve water–energy securities and achieve carbon mitigations in coastal cities. Environ. Sci. Technol. 57, 5068–5078.